Journal of the Optical Society of Korea, Vol. 7, No. 2, June 2003, pp. 106-112

Temperature Compensation of a Strain Sensing Signal from a Fiber Optic Brillouin Optical Time Domain Analysis Sensor

Il-Bum Kwon* and Chi-Yeop Kim

Smart Measurement Group, Korea Research Institute of Standards and Science, Daejeon 305-340, KOREA

Seok-Beom Cho and Jung-Ju Lee

Department of Mechanical Engineering, Korea Advanced Institute of Science and Technology, Daejeon 305-701, KOREA

(Received April 2, 2003)

In order to do continuous health monitoring of large structures, it is necessary that the distributed sensing of strain and temperature of the structures be measured. So, we present the temperature compensation of a signal from a fiber optic BOTDA (Brillouin Optical Time Domain Analysis) sensor. A fiber optic BOTDA sensor has good performance of strain measurement. However, the signal of a fiber optic BOTDA sensor is influenced by strain and temperature. Therefore, we applied an optical fiber on the beam as follows: one part of the fiber, which is sensitive to the strain and the temperature, is bonded on the surface of the beam and another part of the fiber, which is only sensitive to the temperature, is located nearby the strain sensing fiber. Therefore, the strains can be determined from the strain sensing fiber while compensating for the temperature from the temperature sensing fiber. These measured strains were compared with the strains from electrical strain gages. After temperature compensation, it was concluded that the strains from the fiber optic BOTDA sensor had good coincidence with those values of the conventional electrical strain gages.

OCIS code : 060.2370.

I. INTRODUCTION

Fiber optic sensors for the application of smart structures have many advantages in that they are easy to embed in large structures, very sensitive, and can give some distributed information of structures [1]. Especially, the distributed strain and temperature of large structures are to be sensed not only to compensate the temperature effects on the strain measurement but also to evaluate the structural integrity. Many researchers have researched the development of fiber optic distributed sensors. In 1976 Barnoski and Jensen reported a method to measure the loss of light nondestructively by an analysis of Rayleigh back scattering in the time domain [2]. Sensors utilizing stimulated Brillouin scattering have the capability of measuring the absolute physical properties such as strain and temperature. A stimulated Brillouin scattering fiber optic sensor employs a pumping pulse and a CW probe beam running along a single mode optical fiber in opposite directions and detects the stimulated Brillouin back scattering signal amplified by two light beams and acoustic wave mixing [3,4]. In this method the frequency of the CW probe beam differs from the pump beam by the amount of the Brillouin frequency of the optical fiber to enable the amplification and high intensity Brillouin scattering signal to be obtained [5]. The BOTDA sensor system equipped with one electro-optic modulator has been studied for measuring distributed strain and temperature [3].

In this study we investigated the feasibility of the continuous measurement of the distributed strain and temperature on a beam. The fiber optic BOTDA sensor system was developed with one laser diode and two electro-optic modulators. The optical fiber of 16 m was installed on the surface of the beam. The beam

was bent by the self weight and load.

II. OPERATING PRINCIPLE

When the power of the optical pulse signal, which propagates along the single-mode optical fiber, is larger than the Brillouin threshold power, the backward stimulated Brillouin scattering (SBS) signal is generated. SBS can be described as a parametric interaction among the incident light, the Stokes light and an acoustic wave. The Brillouin frequency shift ν_B of the backward scattering light of the light propagating in an optical fiber is expressed as follows [7]:

$$\nu_B = \frac{2nv_A}{\lambda_p} \tag{1}$$

where v_A is the acoustic velocity, n is the effective refractive index, and λ_p is the pump wavelength. The spectral width $\Delta\nu_B$ of the Brillouin gain spectrum is related to the phonon lifetime by the following expression.

$$\Delta\nu_B = (\pi T_B)^{-1} \tag{2}$$

where T_B is the damping time of acoustic waves or the phonon lifetime.

A sensor using this stimulated Brillouin scattering of optical fiber is shown in Fig. 1. The pumping pulse light is launched at $Z = 0$ and propagates in the $+Z$ direction, while the CW probe light is launched at the opposite fiber end ($Z = L$) and propagates in the $-Z$ direction. In this configuration, the pump pulse generates backward Brillouin gain in a single-mode fiber [8]. The center frequency in the Brillouin gain bandwidth is downshifted from the pump frequency ν to the Stokes frequency $\nu - \nu_B$. When the CW probe

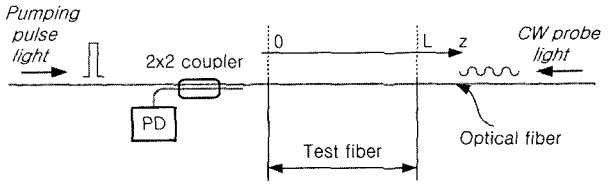

FIG. 1. Schematic diagram for the fiber optic BOTDA sensor operation.

light frequency is in resonance with the Stokes frequency, the CW probe light is amplified through Brillouin interaction with the pump pulse. The amplified CW probe light is passed through the 2 × 2 coupler and is detected by the time-resolved measurement.

The detected power P_d of the CW probe light that arrives at $Z = 0$ is time dependent. The CW probe light amplified at $Z = z$ in the fiber arrives at the fiber end ($Z = 0$) at time $t = 2z/v$ after the injection of the pumping pulse into the fiber. Here, v is the light velocity in the fiber. Therefore, the amplified CW probe light spreads over a period of $2L/v$ for a fiber of length L as shown in Fig. 2. The increment of the power of the CW probe light due to Brillouin interaction is approximately independent of the interaction point in the fiber. However, the CW probe light amplified at $Z = z$ is attenuated by the fiber between $Z = 0$ and $Z = z$. Therefore, the detected signal decays with time. The decay rate with fiber length yields the fiber attenuation coefficient at the CW probe light frequency α_{cw}.

Assuming that the pump pulse has a narrow pulse width W and peak power $P_p(0)$ the power detected at $Z = 0$ at time $t = 2z/v$ can be expressed as

$$P_d(z) = P_{cw}(L)\exp(-\alpha_{cw}L) + (g/A)(vW/2)P_{cw}(L)\exp(-\alpha_{cw}L)P_p(0)\exp(-\alpha_p z) \tag{3}$$

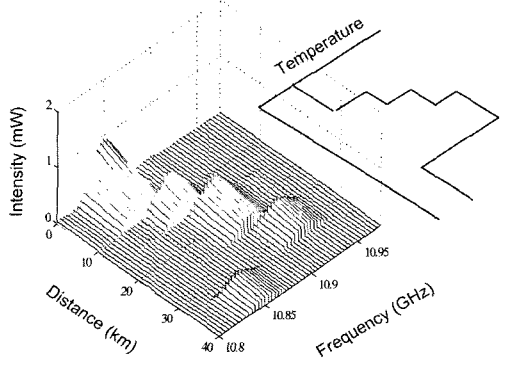

FIG. 2. Simulated signals for backward Brillouin scattering and strain effects.

which is valid for a sufficiently low CW power $P_{cw}(L)$ [8]. In the above expression, g is the Brillouin gain factor, A is the effective cross section of the fiber, and α_p is the optical fiber loss coefficient at the pump pulse wavelength. The Brillouin gain factor g has a well-known expression,

$$g = 2\pi n^2 p_{12}^2 \gamma / c\lambda^2 \rho v_a \Delta\nu_B \tag{4}$$

where n is the refractive index of optical fiber, p_{12} is the photo-elastic constant of the fiber, λ is the wavelength of the optical source, ρ is the fiber density, v_a is the acoustic velocity, $\Delta\nu_B$ is Brillouin gain band-

TABLE 1. Parameters of commercial fiber used in the calculation of Brillouin gain factor.

Parameter	Symbol	Value
Refractive index	ν	1.45
Photoelastic constant	P_{12}	0.29
Density	ρ	2.2×10^3 kg/m^3
Acoustic velocity	v_a	6×10^3 m/s
Brillouin gain bandwidth	$\Delta\nu_B$	13.4 MHz
Polarization factor	γ	0.5

width, and γ is the coefficient of polarization. Table 1 summarizes the values of parameters used in the present calculation of Brillouin gain factor. The wavelength of optical source used in the present study is 1550 nm.

In the first approximation, if Brillouin frequency shift changes linearly with physical parameters such as strain and temperature acting on the fiber, then the temperature from a temperature sensing optical fiber located on structures can be determined from the following equation.

$$\nu_B(T) = \nu_B(0) + C_T T \tag{5}$$

where T is temperature and C_T is the coefficient of temperature, which is known to be 1 MHz/°C for conventional single mode optical fibers used at the 1.5μm wavelength range of the optical communication. Based on the above discussions we calculated a simulation of a strain effect as shown in Fig. 2, which is drawn by the use of W = 30 nsec, $P_p(0)$ = 1341 mW, $P_{cw}(L)$ = 5.7 mW, and L = 40 km into Eq. (3). In this figure, the temperature effect is assumed to induce constant values along three sections of the fiber as shown in Fig. 2. Then, according to the Eq. (5), Brillouin frequency is shifted as the similar pattern of the temperature profile through the fiber length. The temperature effect is shown as a stepwise change of Brillouin frequency in this figure so that both the location and values of the temperature can be determined clearly as the following equation.

$$T = \frac{1}{C_T}\{\nu_B(T) - \nu_B(0)\} \tag{6}$$

If a strain sensing optical fiber is to be bonded on the surface of structures nearby the temperature sensing fiber, then this fiber is to be affected by not only strain but also temperature. So, the Brillouin frequency shift changes by temperature and strain as following equation.

$$\nu_B(\epsilon, T) = \nu_B(\epsilon) + \nu_B(T) \tag{7}$$

The Brillouin frequency shift only affected by the strain effect on the strain sensing fiber is related with the strain as the following equation. It is not included the temperature compensation in this equation.

$$\nu_B(\epsilon) = \nu_B(0) + C_\epsilon \epsilon \tag{8}$$

In order to compensate the temperature effect, Eq. (7) should be inserted in Eq. (8), then the strain after temperature compensation is easily determined by the following equation.

$$\begin{aligned}\epsilon &= \frac{1}{C_\epsilon}\{\nu_B(\epsilon) - \nu_B(0)\} \\ &= \frac{1}{C_\epsilon}\{\nu_B(\epsilon, T) - \nu_B(T) - \nu_B(0)\}\end{aligned} \tag{9}$$

III. SENSOR SETUP AND CALIBRATION

The fiber optic BOTDA sensor consists of an optical source part and a detector part shown in Fig. 3. The optical source part is composed of a DFB diode laser with maximum output of 30 mW and normal bandwidth of 3 MHz, and an optical amplifier of its maximum output of 18 dBm. Pumping pulsed light is generated at the duty cycle of 1 milli-second, and also at the pulse extinction of 20 dB by an electro-optic modulator 1 (EOM1, 2.5 Gb/sec modulation), which is driven by a electric pulse generator. The pumping pulsed light of width, 30 nsec, has been used in this experiment, which corresponds to the spatial resolution of 3 m. The CW probe light is modulated at about

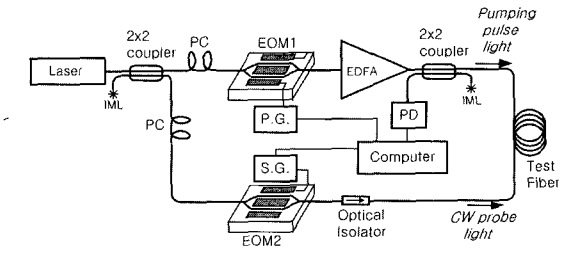

FIG. 3. A schematic diagram of the fiber optic BOTDA sensor.

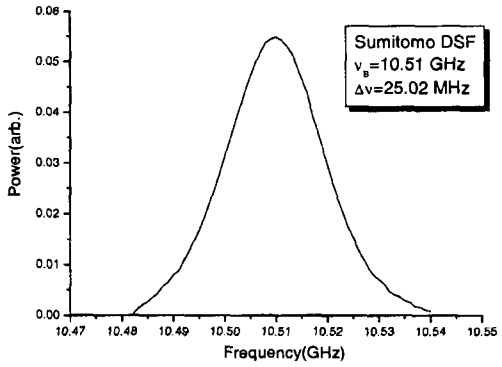

FIG. 4. Brillouin gain spectrum of the single mode optical fiber.

10 GHz range and also at the modulation depth of less than 1 dB by using EOM2 (20 Gb/sec) driven by an electric signal generator. One 50:50 bidirectional fiber coupler was used to divide the light from the DFB laser diode to two lights for a pumping pulsed light and a CW probe light. Another coupler was inserted at the start point of the test fiber to acquire the stimulated Brillouin backward scattering lights. An optical detector was applied to transfer the backward Brillouin light to electric signals and its output data was also transferred to PC by using a high speed A/D converter. When CW pumping light was launched into the fiber with no modulation and the frequency of the CW probe light is swept over near the resonance, we obtained the Brillouin gain spectrum as shown in Fig. 4. From this measurement, we were able to find that the Brillouin frequency shift of the present optical fiber, Sumitomo DSF fiber, is about 10.510 GHz and the bandwidth of spectrum at FWHM is about 25.02 MHz. After constructing the sensor, the calibration test was carried out to determine the strain sensitivity and also the temperature sensitivity. A part, 15 m, of the test fiber, 4 km, was pulled out to expand the length. After pulling the fiber, the strain was going to determine from the expanded length and the Brillouin frequency shift was also measured as shown in Fig. 5. This figure shows Brillouin frequency shift is changed linearly due to strain. According to the same procedure, the strain was related to the Brillouin frequency shift as shown in Fig. 6. In this figure, the strain sensitivity was determined as 467 MHz/100micro-strain. The temperature sensitivity was also determined as 0.98 MHz/°C from a tempera-

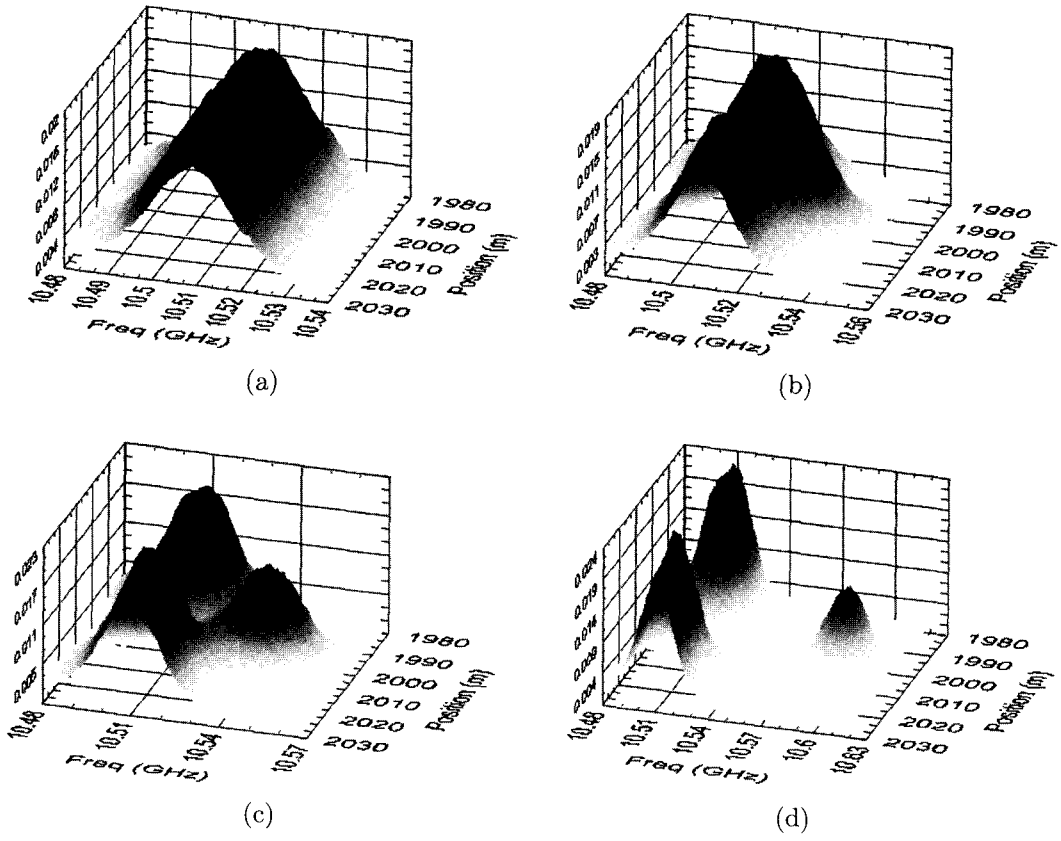

FIG. 5. Brillouin frequency shift according to strain. (a) Strain = 0. (b) Strain = 2.1 micro-strain. (c) Strain = 6.4 micro-strain. (d) Strain = 10.5 micro-strain.

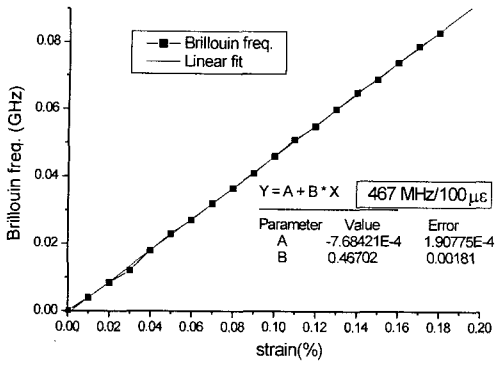

FIG. 6. Strain sensitivity.

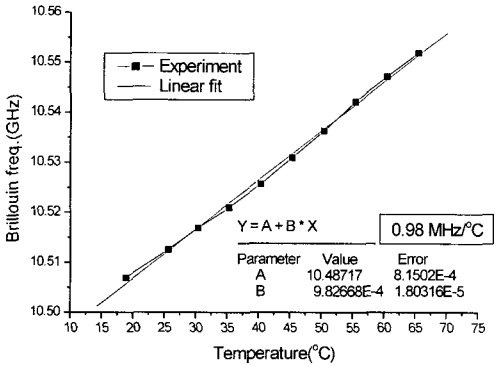

FIG. 7. Temperature sensitivity.

ture chamber test using the 15 m part of the test fiber, 4km as shown in Fig. 7.

IV. BEAM TESTS AND RESULTS

A steel beam, of which length was 8 m, was prepared to be deformed by self weight and a weighting

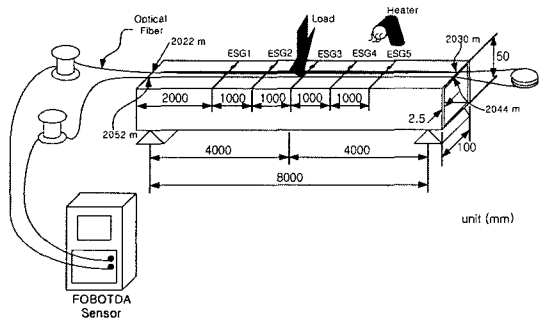

FIG. 8. Experimental setup of a beam with a sensing fiber.

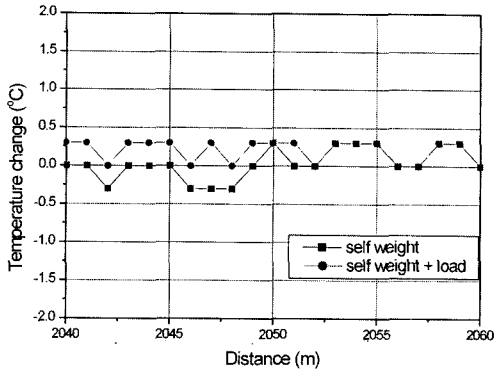

(a)

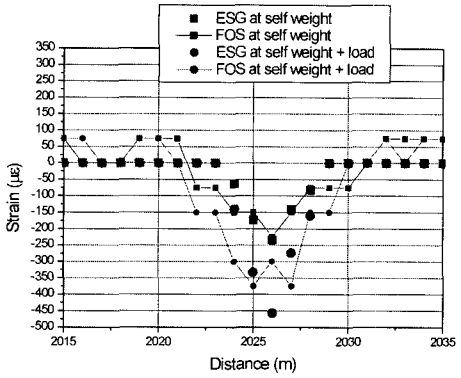

(b)

FIG. 9. Experimental results of the beam at no heating. (a) temperature from temperature sensing fiber. (b) strain from strain sensing fiber.

block (load) as shown in Fig. 8. The strain sensing fiber was bonded on the upper surface of the beam from 2022m to 2030 m, and also the temperature sensing fiber was located from 2044 m to 2052 m by the strain sensing fiber. In Fig. 8, electrical strain gauge was also bonded on the upper surface of the beam. If the beam is to be deformed by loading, then the strain of the upper surface of the beam is to be changed, and also if the heater is to be operated at the right of the beam, then the signal of the strain sensing fiber is to be affected by the temperature change. So, we should compensate the signal of the strain sensing fiber with the signal of the temperature sensing fiber. We could show that the temperature on the upper surface of the beam was constant at the condition of no heating shown in Fig. 9 (a). The strain from the strain sensing fiber of the upper surface of the beam, which was determined by using the strain sensitivity of 4.5 x 467MHz/100microstrain, was compared with the values from the electrical strain gage at no heating condition in Fig. 9 (b). The strain sensitivity of the fiber

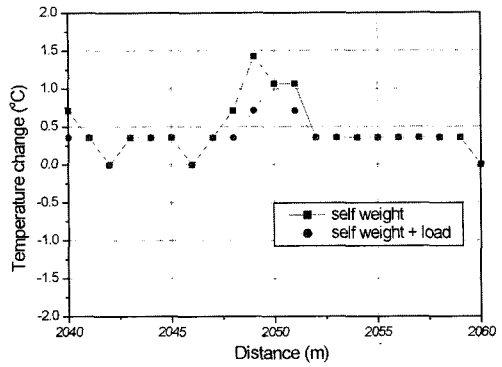

(a)

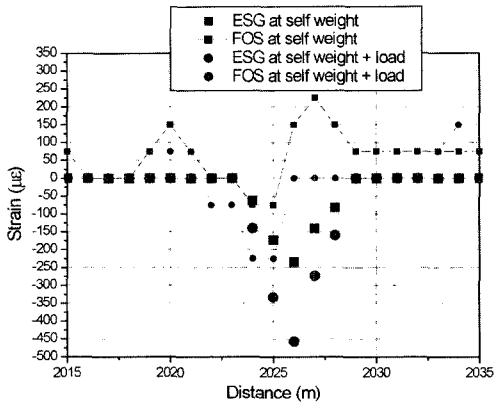

(b)

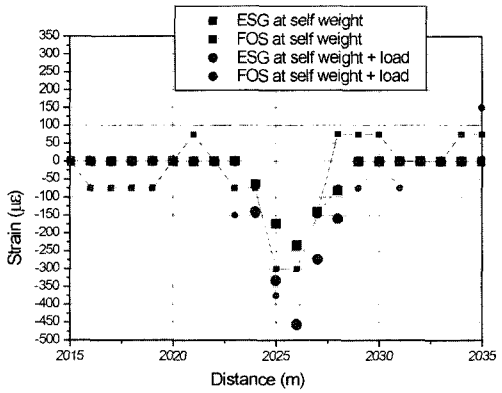

(c)

FIG. 10. Experimental results of the beam at heating. (a) temperature from temperature sensing fiber. (b) strain from strain sensing fiber (before compensation). (c) strain from strain sensing fiber (after compensation).

sensor was increased to compensate the average value of the strain distributed on the optical fiber. The temperature of the upper surface of the beam was changed at the condition of heating as shown in Fig. 10 (a). In that case, the strain from the strain sensing fiber, which is determined by Eq. (8), was not correlated with the strain from the electrical strain gauge as shown in Fig. 10 (b). So, in order to determine the true strain, the strain data should be compensated by the temperature data according to Eq. (9). After the temperature compensation, the difference between the strain from the optical fiber and the strain from the electrical strain gage was less than the difference of the strains before compensation as shown in Fig. 10 (c).

V. CONCLUSION

The feasibility of the continuous measurement of the distributed strain and temperature was investigated by performing the beam test. The fiber optic BOTDA sensor system was developed with one laser diode and two electro-optic modulators. The strain sensing optical fiber of 8 m was bonded on the surface of the beam, and also the temperature sensing fiber was located nearby the strain sensing fiber. From the test, the strains from the strain sensing fiber were compensated with the strains from the electrical strain gages after temperature compensation. The differences between the strain of the fiber sensor and the strain of the electrical strain gage was less than the differences before compensation. In future study, we will investigate the compensation error on the strain measurement by fiber optic BOTDA sensor.

*Corresponding author : ibkwon@kriss.re.kr.

REFERENCES

[1] R. O. Claus, J. C. Mckeeman, R. G. May, and K. D. Bennet, "Optical Fiber Sensors and Signal Processing for Smart Materials and Structures Applications." *Structures and Mathematical Issues Workshop*, Proc. of ARO Smart Materials, pp. 29-38, 1988.

[2] M. K. Barnoski and S. M. Jensen, *Applied Optics*, Vol. 15, No. 9, pp. 2112-2115, Sept. 1976.

[3] M. Nickles, L. Thevenaz, and P. Robert, "Simple distributed fiber sensor based on Brillouin gain spectrum analysis," *Optics Letters*, Vol. 21, No. 10, pp.758-760, 1996.

[4] V. Lecoeuche, D. J. Webb, C. N. Pannel, and D. A. Jackson, "Brillouin Based Distributed Fibre Sensor Incorporating a Mode-locked Brillouin Fibre Ring Laser," *Optics Communications*, Vol.152, pp. 263-268, 1998.

[5] L. Thevenaz, M. Facchini, A. Fellay, and P. Robert, "Monitoring of large structure using distributed Brillouin scattering fiber sensing," *OFS-13*, pp.345-348, 1999.

[6] G. P. Agrawal, *Nonlinear Fiber Optics*, (Academic press, New York, 2nd ed., 1995), pp.370-378.

[7] T. Horiguchi and M. Tateta, "BOTDA-Nondestructive Measurement of Single-mode Optical Fiber Attenuation Characteristics Using Brillouin Interaction Theory," *Journal of Lightwave Technology*, Vol. 7, No. 8, pp.1170-1176, 1989.

[8] I. B. Kwon, M. Choi, J. Yu, and S. Baik, "Development of fiber optic BOTDA sensor," *Hankook Kwanghak Hoeji*, Vol. 12, No. 4, pp. 294-299 (in Korean), 2001.